Multichain Aggregates in Dilute Solutions of Associating Polyelectrolyte Keeping a Constant Size at the Increase in the Chain Length of Individual Macromolecules

Evgeniya V. Korchagina and Olga E. Philippova*

Physics Department, Moscow State University, Moscow 119991, Russia

Received August 23, 2010; Revised Manuscript Received October 25, 2010

Multichain aggregates together with individual macromolecules were detected by light scattering in dilute aqueous solutions of chitosan and of its hydrophobic derivatives bearing 4 mol % of *n*-dodecyl side groups. It was demonstrated that the size of aggregates and their aggregation numbers increase at the introduction of hydrophobic side groups into polymer chains. The key result concerns the effect of the chain length of individual macromolecules on the aggregation behavior. It was shown that for both unmodified and hydrophobically modified (HM) chitosan, the size of aggregates is independent of the length of single chains, which may result from the electrostatic nature of the stabilization of aggregates. At the same time, the number of macromolecules in one aggregate increases significantly with decreasing length of single chains to provide a sufficient number of associating groups to stabilize the aggregate. The analysis of the light scattering data together with TEM results suggests that the aggregates of chitosan and HM chitosan represent spherical hydrogel particles with denser core and looser shell covered with dangling chains.

Introduction

Study of the self-assembly of associating polyelectrolytes in dilute solutions is quite important for the preparation of new functional polymeric systems. For instance, multichain aggregates of nontoxic, biocompatible, and biodegradable polymers are very promising for various applications in pharmacy, biotechnology, cosmetics, and so on.[1,2] In particular, it concerns aggregates formed by chitosan and its hydrophobic derivatives.

Chitosan, a (1→4)-linked linear copolymer of 2-amino-2-deoxy-β-D-glucan (GlcN) and 2-acetamido-2-deoxy-β-D-glucan (GlcNAc), is produced commercially by alkali N-deacetylation of chitin, the second most abundant polysaccharide in nature after cellulose.[3] Chitosan is soluble in water at acidic pH (pH <6), when most of the amino groups are protonated. Chitosan is characterized by its degree of acetylation, that is, the average molar fraction of GlcNAc units remaining upon incomplete chemical modification of chitin. These units were shown to play an important role in the self-aggregation of chitosan macromolecules.[4] Depending on its source and composition, the chitosan samples behave differently in aqueous acidic medium: in some cases, they form molecularly dispersed solutions;[5−9] in other cases, they form aggregates.[4,10−15] The reason for this behavior is not yet understood.

Introduction of hydrophobic side groups in chitosan chains significantly enhances their tendency to self-association in water. Similar to any other hydrophobically associating polyelectrolyte, protonated HM chitosan that is dissolved in water should spontaneously form aggregates of some optimum size determined by the competition of hydrophobic association inducing growth of aggregates and electrostatic repulsion limiting their growth.[16,17] By playing with these counteracting effects, one may easily obtain rather monodisperse aggregates of the desired size. If necessary, the spontaneously formed aggregates may be stabilized by covalent cross-linking, for example, by glutaraldehyde.[18−22] Multichain aggregates of HM chitosan are very promising as carriers for drug delivery, especially for hydrophobic drugs. Positive charge of these species can enhance their penetration through cell membranes and thus provide mucoadhesive and antimicrobial properties.[1,2,23−27] Also, multichain aggregates of HM chitosan have high potential as gene carriers[1,28] because the presence of hydrophobic moieties may improve the transfection.[29]

Recently, the studies of the self-aggregation behavior in dilute aqueous solutions were performed with various HM chitosan samples[5,7,9,12,30−39] including those with alkyl,[9,12,32,39] octanoyl,[35] palmitoyl,[34,35] stearoyl,[35,37] linoleyl,[33] oleoyl,[38] deoxycholic acid,[5,7,31] and cholesterol substituents.[36] Most of attention was paid to the investigation of the self-assembly of hydrophobic substituents by fluorescence probe method.[5,7,9,12,31,33−39] In some papers,[5,31,34,35,38] the effect of the content of hydrophobes on the size of multichain aggregates was studied. At the same time, the impact of such an important parameter as the main chain length of HM chitosan on the dimensions of aggregates is not yet understood. Also, little is known[7,32] about the aggregation numbers of multichain aggregates.

The aim of the present Article is to study the effect of the chain length of chitosan and HM chitosan macromolecules on the size and on the aggregation numbers of multichain aggregates formed in dilute aqueous solutions of these polymers.

Experimental Section

1. Materials. Chitosan (Chart 1) was obtained by alkaline N-deacetylation of chitin from Far East crab shells and purified from metal salts by repeated precipitation from 1 M HCl solution to 2 M NaOH and washing of the precipitate by distilled water as described in detail in ref 40. The degree of acetylation of chitosan samples was determined by potentiometry and ^{1}H NMR as reported elsewhere[41] and found to be equal to 0.05.

The chitosan samples with different molecular weights were obtained by acid hydrolysis of the initial chitosan sample in homogeneous

* To whom correspondence should be addressed. E-mail: phil@polly.phys.msu.ru.

10.1021/bm100990u
Published on Web 11/24/2010

Chart 1. Chemical Structure of (a) Chitosan and (b) HM Chitosan

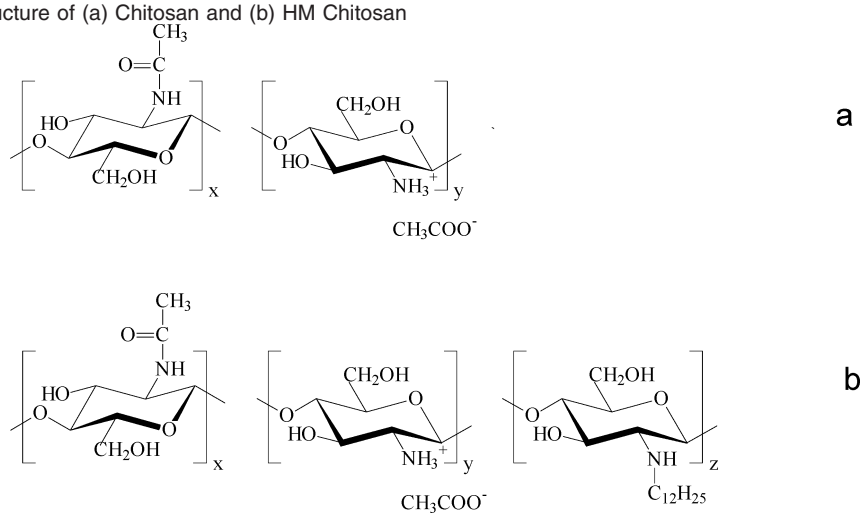

Table 1. Characteristics of Chitosan Used in This Study

sample	M_{uni} (g/mol)	degree of polymerization P	contour length L (nm)[a]
chitosan 55	55 000	340	175
chitosan 70	70 000	430	220
chitosan 125	125 000	770	395

[a] L is calculated as 0.515 P, where 0.515 nm is the repeat unit projection on the main chain,[43,44] and P is the degree of polymerization.

medium. Each of the samples was further purified by fractional precipitation.[42] The M_w values of the prepared samples were estimated by static light scattering (SLS) under the conditions, when the self-aggregation is essentially suppressed. These conditions include the use of 0.3 M CH_3COOH/0.2 M CH_3COONH_4 as a solvent breaking the interchain hydrogen bonds in chitosan solutions[13,14] and the measurements *immediately* after filtration through 0.1 μm filter. In this case, the aggregates destroyed at the filtration do not have enough time to be reformed. The values of M_w thus obtained are presented in Table 1. The kinetic evolution of the aggregate formation in 0.3 M CH_3COOH/0.2 M CH_3COONH_4 will be described in detail in a separate paper.

The HM chitosan samples were prepared by reductive amination of the three chitosan samples with different M_w in homogeneous conditions using *n*-dodecylaldehyde.[45] The content of hydrophobic *n*-dodecyl groups in all HM chitosans was found to be equal to 4 mol % according to ^{1}H NMR data. The hydrophobic modification did not affect the degree of polymerization of the polysaccharide.

2. Sample Preparation. For the study of aggregation, acetate buffer 0.3 M CH_3COOH/0.05 CH_3COONa was used as a solvent. Stock solutions of chitosan were prepared by slow dropwise addition of a solvent filtered through a 0.22 μm Millipore Millex-LCR filter to chitosan powder. To ensure a complete dissolution of polymer, we stirred the solutions at room temperature for a few days; then, they were filtered through a 0.45 μm Millipore Millex-LCR filter. The possible loss of matter in the filtration stage was evaluated by quantitative determination of chitosan concentration before and after filtration with ninhydrin method.[46−48] It was shown that the amount of lost polymer does not exceed 2%. We prepared sample solutions with concentrations of 0.05 to 1.5 g/L by mixing appropriate amounts of stock solution and filtered solvent.

It was found that in 0.3 M CH_3COOH/0.05 M CH_3COONa the amino groups of chitosan are fully protonated.[49] Under these conditions, the mean distance between the charged units in the macromolecules of chitosan is ca. 5.5 Å.[4] The characteristic length of the electrostatic interactions (the Debye−Hückel length r_D) in the solvent under study was estimated with the formula[50]

$$r_D = \sqrt{\varepsilon_0 \varepsilon k_B T / 4\pi e^2 (^1/_2 \sum c_i z_i^2)} \quad (1)$$

where k is the dielectric constant, k_B is the Boltzmann constant, T is the absolute temperature, e is the elementary charge, $(^1/_2 \sum c_i z_i^2)$ is the ionic strength of solution, and c_i and z_i are the concentration and the valence of ions of a given type, respectively. When calculating the ionic strength, only the contribution of sodium acetate was taken into account, whereas the input of dissociated acetic acid was neglected. It was shown that the Debye−Hückel length r_D is equal to ca. 13.6 Å, which is 2.5 times larger than the average distance between the charged units of chitosan. This indicates that added salt does not completely screen the electrostatic interactions in the system.

3. Light Scattering Measurements. SLS and dynamic light scattering (DLS) experiments were performed on an ALV/DLS/SLS-5000 compact goniometer system equipped with an ALV digital time correlator, helium−neon laser operating at a wavelength of 632.8 nm, and computer-controlled and stepping-motor-driven variable-angle detection system. The incident light was vertically polarized with respect to the scattering plane, and the light intensity was regulated with a beam attenuator.

In the SLS experiments, the angular dependence of the excess absolute time-average scattered intensity with respect to the solvent, that is, Rayleigh ratio R_θ (q), was measured. Toluene was used as a reference standard. The scattering angle θ was varied from 30 to 150°.

For a dilute polymer solution at a relatively small scattering angle θ, Rayleigh ratio R_θ is related to the weight-average molecular weight M_w, the second virial coefficient A_2, and the z-average radius of gyration R_g via the following expression[51]

$$\frac{KC}{R_\theta} \approx \frac{1}{M_w}\left(1 + \frac{1}{3}R_g^2 q^2\right) + 2A_2 C \quad (2)$$

where C is the polymer concentration, $K = 4\pi^2 n^2 (dn/dc)^2 / N_A \lambda^4$ is the scattering constant, and $q = 4\pi n/\lambda \sin(\theta/2)$ is the scattering vector. Here N_A is Avogadro's number, λ is the wavelength of light in vacuum, n is the refractive index of solvent, and dn/dc is the refractive index increment. For convenience, the abbreviation $R_g \equiv (\langle R_g^2 \rangle_z)^{1/2}$ is used.

According to eq 2, the extrapolation $(KC/R_\theta)_{c\to 0, q\to 0}$ gives the $1/M_w$ value, whereas the slopes of $(KC/R_\theta)_{c\to 0}$ versus q^2 and $(KC/R_\theta)_{q\to 0}$ versus C lead to R_g and A_2 values, respectively.

In DLS experiments, the normalized time autocorrelation function $g^{(2)}(q,t)$ of the scattered intensity is measured.[6]

$$g^{(2)}(q,t) = \frac{\langle I(q,t) I(q,0) \rangle}{\langle I(q,0) \rangle^2} \quad (3)$$

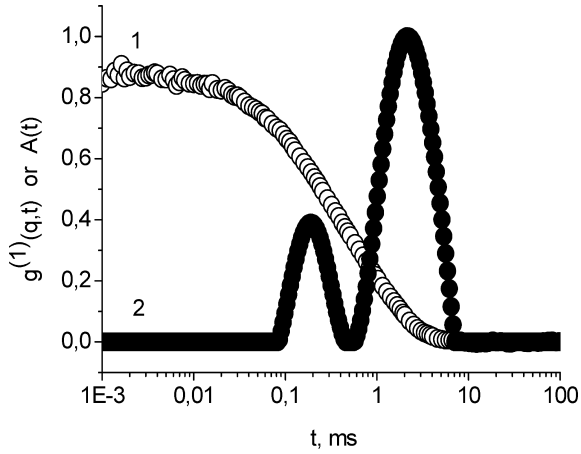

Figure 1. (1) Semilog representation of the field autocorrelation function $g^{(1)}(q,t)$ at scattering angle $\theta = 90°$ for 0.4 g/L aqueous solution of chitosan (125 000 g/mol). (2) Distribution function of decay time $A(t)$ obtained by Contin method for the same sample. The fast peak corresponds to single coils, and the slow peak corresponds to the aggregates. Solvent: 0.3 M acetic acid/0.05 M sodium acetate.

where $I(q,0)$ and $I(q,t)$ are the scattering intensities at time $t = 0$ and at a certain delay time t later.

It is related to the field autocorrelation function (or the autocorrelation function of the concentration fluctuations) $g^{(1)}(q,t)$ through $g^{(2)}(q,t) = A + \beta|g^{(1)}(q,t)|^2$, where A is the baseline and β is the coherence factor.

To obtain the relaxation time distribution, we applied the Contin analysis. It is based on the Laplace inversion of $g^{(1)}(q,t)$.[52] In the case when the spectral profile of the scattered light can be described by a multi-Lorentzian curve, $g^{(1)}(q,t)$ can be written as

$$g^{(1)}(q,t) = \int_0^\infty G(\Gamma)\exp(-\Gamma t)\,d\Gamma \qquad (4)$$

where Γ is the decay rate and $G(\Gamma)$ is the normalized decay constant distribution. This method is more appropriate for solutions characterized by several relaxation mechanisms.[6]

For a diffusive relaxation, Γ is related to the translational diffusion coefficient D by $(\Gamma/q^2)_{c\to 0,\, q\to 0} = D$, so that $G(\Gamma)$ can be converted into a translational diffusion coefficient distribution or a hydrodynamic radius distribution by using the Stokes−Einstein equation valid for spheres

$$R_h = k_B T/6\pi\eta_s D \qquad (5)$$

where η_s is the solvent viscosity.

4. Refractive Index Increment Determination. The refractive index increment dn/dc value was determined for solutions of unmodified chitosan sample (70 000 g/mol) in 0.3 M CH_3COOH/0.05 M CH_3COONa. The measurements were made with a differential interferometer operating at a wavelength of 632.8 nm. Nine solutions (parent solution and eight dilutions) were analyzed to determine value of dn/dc. The refractive index increment dn/dc value thus obtained was equal to 0.195. Similar values of dn/dc for chitosan in the same solvent 0.3 M CH_3COOH/0.05 M CH_3COONa were found in ref 6. This value was taken for all chitosan samples because it was shown that dn/dc is independent of the molecular weight[53] and the content of hydrophobic groups.[54−56]

5. Transmission Electron Microscopy (TEM) Measurements. Electron micrographs of aggregates of chitosan and HM chitosan were obtained with a LEO912 AB OMEGA transmission electron microscope at the accelerating voltage of 100 kV. The samples for TEM observations were prepared as follows. First, 2.5 μL of 0.05% (w/v) polymer solution in 0.3 M acetic acid was deposited on a 140 mesh Formvar-coated copper grid and dried for 1 min. The excess of solution was blotted off. Then, 2.5 μL of staining solution was added to the top of the sample, blotted off, and dried in the air. In this study, the following heavy metal stains were used: uranyl acetate (1 wt % solution in water at pH 4.5) or an organo-tungstate compound NANO-W provided by Nanoprobes (2 wt % solution in water at pH 6.8). Some samples were examined without staining.

Table 2. Hydrodynamic Radii of Unimers $R_{h\,uni}$ and Aggregates $R_{h\,agg}$ and the Weight Fraction of Aggregates x in Dilute Aqueous Solutions of Chitosan[a]

sample	$R_{h\,uni\,exper}$ (nm)[b]	$R_{h\,uni\,theor}$ (nm)[c]	$R_{h\,agg}$ (nm)[b]	x[b]
chitosan 55	13 ± 2	13	134 ± 5	0.07
chitosan 70	15 ± 2	15	135 ± 8	0.08
chitosan 125	18 ± 2	20	132 ± 9	0.09

[a] Solvent: 0.3 M acetic acid/0.05 M sodium acetate. [b] Values are extrapolated to zero concentration of chitosan. [c] Theoretical estimates of the hydrodynamic radii R_h of coils of individual chitosan macromolecules under θ conditions.

Results and Discussion

Unmodified Chitosan. In the dilute regime, the solutions of chitosan were investigated by DLS. For all samples under study, the correlation functions $g^{(1)}(q,t)$ of polymer concentration fluctuations show a bimodal relaxation behavior with fast and slow relaxation modes (Figure 1)

$$g^{(1)}(q,t) = A_{fast}\exp\left(-\frac{t}{\tau_{fast}}\right) + A_{slow}\exp\left(-\frac{t}{\tau_{slow}}\right) \qquad (6)$$

Here τ_{fast} and τ_{slow} are the fast and slow relaxation times, respectively, and A_{fast} and A_{slow} are the corresponding amplitudes.

The scattering data do not change when the measurements in 0.3 M CH_3COOH/0.05 M CH_3COONa are performed 10 min, 1 h, 24 h, and 1 month after chitosan dissolution and filtration. The plots of the relaxation rates Γ (i.e., the reciprocal of the relaxation time) for the fast and slow modes as a function of the square of scattering vector q^2 yielded straight lines passing through the origin (Figure 2), indicating that both the fast and slow relaxation modes are due to the translational diffusion of particles. The apparent diffusion coefficients D_{app} of the particles estimated from the slope of Γ (q^2) plots were extrapolated to zero polymer concentration. From the obtained values of the diffusion coefficients D at infinite dilution, the hydrodynamic radii of the particles were calculated using the Einstein−Stokes equation (eq 5). The results obtained are summarized in Table 2.

To attribute the modes, the theoretical estimations of hydrodynamic radii of individual chains under θ conditions were made according to the expression[50]

$$R_h \approx (3\pi/128)^{1/2}\cdot(2L\cdot l_p)^{1/2} \qquad (7)$$

where l_p is the persistence length (the value of 7.5 nm was taken for chitosan[14]) and L is the contour length.

The theoretical estimates thus obtained are presented in Table 2. It is seen that they are close to the size of smaller particles responsible for the fast relaxation mode. Therefore, the fast mode can be attributed to the diffusion of single chitosan macromolecules (unimers). It is reasonable to suggest that larger particles responsible for the slow relaxation mode are intermolecular aggregates. This suggestion is supported by the fact that at

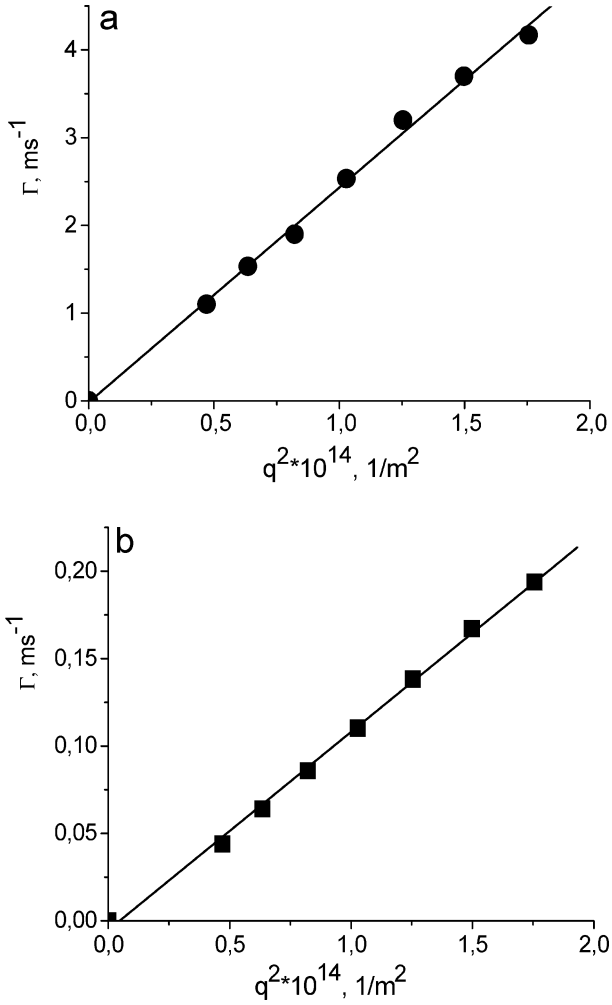

Figure 2. Relaxation rate (reciprocal of the relaxation time) as a function of the square of scattering vector q^2 for (a) fast and (b) slow modes for 0.85 g/L aqueous solution of chitosan (55 000 g/mol). Solvent: 0.3 M acetic acid/0.05 M sodium acetate.

dilution the scattering intensity provided by single macromolecules increases with respect to that of larger particles (Figure 3), which may be explained by the shift of the dynamic equilibrium between single chains and multichain aggregates toward single chains due to increasing gain in entropy at the release of unimers from the aggregates to the large volume of external solution.

Therefore, the DLS data show that the dilute aqueous solutions of all samples under study contain both unimers and aggregates of macromolecules even until concentrations of chitosan as low as 0.05 g/L.

The data reported in Figure 1 provide the fraction of scattering intensity arising from particles having a given hydrodynamic radius (so-called unweighted or intensity weighted size distribution). Because light scattering intensity increases strongly with particle size, a few big particles can yield a large light scattering intensity. To get information about the weight fraction of each type of particle in chitosan solution, we can use the following relationship

$$x_i = \frac{w_i/R_{h\,i}^2}{\sum_i (w_i/R_{h\,i}^2)} \qquad (8)$$

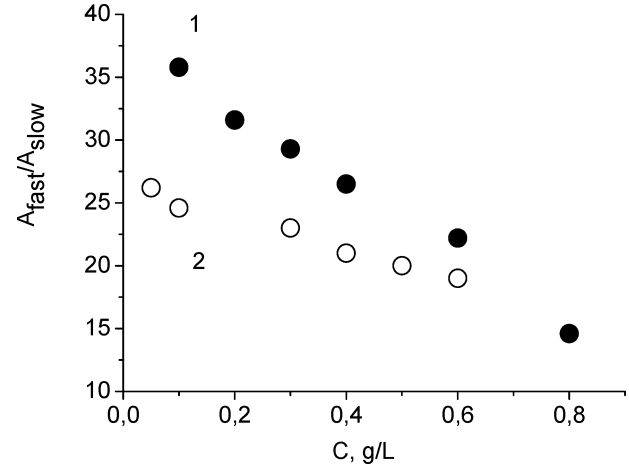

Figure 3. Dependence of the ratio of the amplitude of fast and slow modes A_{fast}/A_{slow} of the electric field autocorrelation function on the concentration of chitosan samples of two different molecular weights (1) 55 000 and (2) 125 000 g/mol at scattering angle 90°. Solvent: 0.3 M acetic acid/0.05 M sodium acetate.

where w_i is the intensity weighed peak area and $R_{h\,i}$ is the hydrodynamic radius of the corresponding particle. Often the exponent in this equation is equal to 3, which corresponds to the case of hard spheres.[57] In our system, the exponent 2 inherent to polymer coils in θ-solvent[50] seems to be more appropriate. The weight fractions of the aggregates thus obtained are summarized in Table 2. It is seen that they are rather small for all samples under study. Close value of the weight fraction of aggregates (ca. 0.05) was obtained by Anthonsen et al.[11] from the data of gel permeation chromatography coupled to low-angle laser light scattering and differential refractive index detectors. Therefore, dilute aqueous solutions of chitosan contain mainly molecular dispersed coils, whereas the fraction of the aggregates is small. The intermolecular aggregates in dilute aqueous solutions were previously observed in many polysaccharides, for example, in dextran,[57] hydroxypropylcellulose,[58] and pectin.[59−62] In all cases, the fraction of aggregates was rather low, but because of the large size of the aggregates, their contribution to the scattering is very significant and should be analyzed.

The values of the hydrodynamic radii of the aggregates are summarized in Table 2 for different polymeric samples. It is seen that the radius $R_{h\,agg}$ of aggregates does not depend on the length of individual chitosan chains. This is one of the most important observations made in this work. It should be noted that for molecularly dispersed (nonaggregated) linear chains, the $R_{h\,uni}$ values scale with molecular weight M_w as $R_{h\,uni} \approx KM_w^{\nu}$, where the value of the exponent ν can vary from $\nu = 0.33$ for the hard spheres to $\nu = 1$ for rigid rods.[63] A value of $\nu = 0.50$ refers to Gaussian coil under θ conditions.[63] As for the $R_{h\,agg}$ values of aggregates, they also increase with increasing molecular weight of individual macromolecules[7,64,65] but less markedly than in the case of unimers. To the best of our knowledge, the present Article for the first time demonstrates that the size of aggregates can be independent of the chain length of individual macromolecules. Such behavior is most probably due to the presence of unscreened charges on the polymer chains. Although the experiments were performed in salt solutions, the amount of added salt was insufficient to screen long-range electrostatic repulsions, which is evident from the fact that the Debye−Hückel length r_D is 2.5 times larger than the average distance between the charged units. (See the calculations in the Experimental Section.)

Table 3. Apparent Weight-Average Molecular Weight (M_w*), Apparent *z*-Average Radius of Gyration (R_g*), and Second Virial Coefficient (A_2) Values Determined from Zimm Plots for Dilute Aqueous Solutions of Chitosan[a]

sample	M_w* (g/mol)	R_g* (nm)	A_2 (cm^3 mol/g^2)
chitosan 55	125 000	69 ± 3	8×10^{-4}
chitosan 70	150 000	68 ± 3	5×10^{-4}
chitosan 125	220 000	66 ± 3	4×10^{-4}

[a] Solvent: 0.3 M acetic acid/0.05 M sodium acetate.

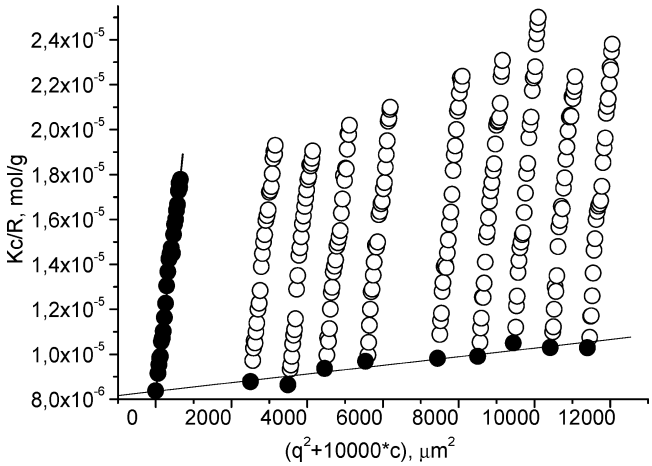

Figure 4. Zimm plot for aqueous solutions of chitosan (55 000 g/mol) in the range of polymer concentrations 0.25 to 1.14 g/L at scattering angles from 35 to 150° at 25 °C. Solvent: 0.3 M acetic acid/0.05 M sodium acetate.

The results obtained are in good agreement with theoretical predictions. Indeed, for dilute solutions of associating polyelectrolytes, the equilibrium mean-field theory developed by Potemkin et al. demonstrates[17] that the size of aggregates is determined only by the content of associating groups and charged units as well as by the fraction of counterions escaped from the aggregate. At the same time, the size of aggregates should be independent of the chain length of individual macromolecules.[17] This result follows from the electrostatic nature of stabilization of the aggregates and is related to the classical Rayleigh problem of the charged droplet: a spherical droplet whose charge exceeds some critical value disintegrates into a set of smaller droplets of a certain size carrying charge lower than the critical one.[66]

To determine the molecular weight of the aggregates M_{agg} and their aggregation numbers N_{agg}, we used the combination of DLS and SLS techniques. Figure 4 shows a typical Zimm plot for chitosan solution. It is seen that the angular dependences of the scattering are essentially linear in the angular range 35−150°. From the Zimm plots, the values of the apparent weight-average molecular weight M_w*, the apparent radius of gyration R_g*, and the second virial coefficient A_2 were determined. They are collected in Table 3.

It is seen that the apparent molecular weights of chitosan samples M_w* are much higher than those of unimers, indicating the presence of aggregates. The values of M_w* can be expressed in terms of the weight-average molecular weights of unimers M_{uni} and aggregates M_{agg} as follows[67,68]

$$M_w^* = (1 - x)M_{uni} + xM_{agg} \quad (9)$$

where x is the weight fraction of the aggregates.

To extract the molecular weight of aggregates M_{agg}, the values of the weight fractions of unimers and aggregates obtained from DLS data should be used (Table 2). The M_{agg} values thus obtained are collected in Table 4. To the best of our knowledge, this is the first estimation of the molecular weight of aggregates in dilute solutions of chitosan. On the basis of the values of M_{agg}, the aggregation numbers N_{agg} were calculated as M_{agg}/M_{uni}.

Table 4. Characteristics of Aggregates in Dilute Aqueous Solutions of Chitosan[a]

sample	M_{agg} 10^6 g/mol	N_{agg}[b]	n_{agg}[c]	$R_{g\,agg}$ (nm)	$(R_g/R_h)_{agg}$	φ_{agg} 10^{-3}
chitosan 55	1.1	20 ± 3	6750	87	0.65 ± 0.05	0.38
chitosan 70	1.1	16 ± 3	6750	87	0.64 ± 0.05	0.38
chitosan 125	1.2	10 ± 2	7300	89	0.67 ± 0.05	0.38

[a] Solvent: 0.3 M acetic acid/0.05 M sodium acetate. [b] Number of polymer chains in one aggregate. [c] Number of monomer units in one aggregate.

The values of the apparent *z*-average radii of gyration R_g* also contain the contributions of both unimers and aggregates. From R_g* values, we obtained the radii of gyration of aggregates $R_{g\,agg}$ by using the following formula[67]

$$R_g^{*2} = \frac{(1 - x)M_{uni}R_{g\,uni}^2 + xM_{agg}R_{g\,agg}^2}{(1 - x)M_{uni} + xM_{agg}} \quad (10)$$

From the values of molecular weight of aggregates M_{agg} and their radii of gyration $R_{g\,agg}$, the polymer volume fraction φ_{agg} in the aggregates was estimated according to the following equation[69] under the assumption that the aggregates can be regarded as homogeneous spheres

$$\varphi_{agg} = \frac{\bar{v}M_{agg}}{N_A(4\pi/3)R_{g\,agg}^3} \quad (11)$$

where $\bar{v}$ is the specific volume of chitosan. ($\bar{v}$ was taken equal to 0.57 mL/g according to ref 70.)

The values of the aggregation numbers N_{agg}, of the radii of gyration of aggregates $R_{g\,agg}$, and of the volume fraction of polymer in the aggregates φ_{agg} thus obtained are given in Table 4. It is seen that the radii of gyration of aggregates $R_{g\,agg}$ are independent of the molecular weight of chitosan. This is in contrast with the behavior of nonaggregated chitosan, for which the radius of gyration increases with molecular weight according to the empirical law:[71] $R_{g,z} = 0.075M_w^{0.55}$. As was discussed above, the independence of the size of aggregates of polyelectrolyte macromolecules on the molecular weight of individual chains comes from the electrostatic nature of stabilization of aggregates, which cannot carry a charge larger than a critical one.

Table 4 shows that the aggregation number drops with increasing length of individual polymer chains, which is in perfect agreement with the theoretical predictions.[17] This result can be explained as follows. The energy of association is determined by the number of attracting groups. Because shorter polymer chains have a smaller number of associating groups, their aggregates should include more chains to get a necessary gain in the energy of association. The most interesting observation consists of the fact that despite the two-fold difference in aggregation numbers, all aggregates are equal in size (see $R_{h\,agg}$ values in Table 2 and $R_{g\,agg}$ values in Table 4), and this result is consistent with the theory of associating polyelectrolytes.[17]

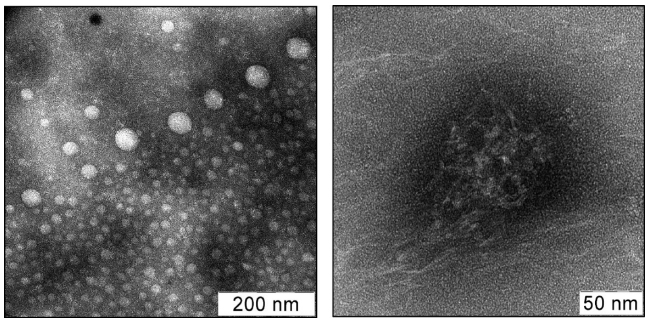

Figure 5. TEM micrographs of multichain aggregates of chitosan (70 000 g/mol) negatively stained with uranyl acetate (left) and organotungstate compound NANO-W (right).

Therefore, chitosan demonstrates a behavior typical for any associating polyelectrolyte. It may be due to the combination of two types of units in chitosan chains: (1) protonated GlcN units responsible for polyelectrolyte properties and (2) uncharged GlcNAc units, which can be considered as hydrophobic attracting sites. The attraction may also be due to hydrogen bonding.[13] In this case, both types of repeat units can be involved in the association process.[12] One can suggest that the aggregates of chitosan can be regarded as nanogels, where the cross-links represent junction zones[12] between different chains, which are formed because of hydrophobic interactions, hydrogen bonding, or both.

To get insight into the form of aggregates, the values of the ratio R_g/R_h and the volume fraction of polymer in aggregate φ_{agg} were considered. Table 4 shows that the R_g/R_h values for the aggregates of chitosan are quite small (0.64 to 0.67), even below the "hard sphere" R_g/R_h value (0.778).[72] According to refs 72 and 73, small R_g/R_h values may be observed in microgels covered with dangling chains, which give a larger hydrodynamic radii than a "hard sphere" with its well-defined surface. Table 4 shows that the volume fraction of polymer in aggregate φ_{agg} is ca. 0.38×10^{-3}, which is only two to four times higher than the theoretical estimation of the volume fraction of the corresponding nonaggregated chains in a coil swollen in a good solvent, indicating that the aggregates are very loose.

To visualize the aggregates of chitosan, TEM was used. Typical pictures obtained are presented in Figure 5. It is seen that the aggregates are of nearly spherical shape and contain brighter core and darker shell when negatively stained. Darker shell may indicate that it is loose, and some of stain molecules can easily penetrate it. Therefore, the TEM observations are consistent with the suggestions made on the basis of LS data.

The average radius of the aggregates on TEM images is much lower than the $R_{h\,agg}$ value obtained by DLS (135 nm), which is expected taking into account a low polymer volume fraction in the aggregate and the fact that TEM visualizes the dried aggregates on the surface, whereas DLS deals with highly swollen aggregates in the solvent.

It should be noted that the aggregation behavior depends significantly on the composition and source of chitosan sample. Indeed, in some papers, no aggregation was detected in dilute solutions of chitosan.[6,8,74] In particular, in ref 6, only single molecules with R_h of 49 nm were observed by DLS in dilute solutions of chitosan ($DA = 0.12$, $M_w = 190\,000$ g/mol) in the same solvent (0.3 M acetic acid/0.05 M sodium acetate). Under these conditions, the A_2 value was shown to be on the order of 10^{-3} cm^3 g^{-2} mol with a positive sign, which is evidence that 0.3 M acetic acid/0.05 M sodium acetate is a good solvent for the chitosan sample they studied. We made a theoretical estimate

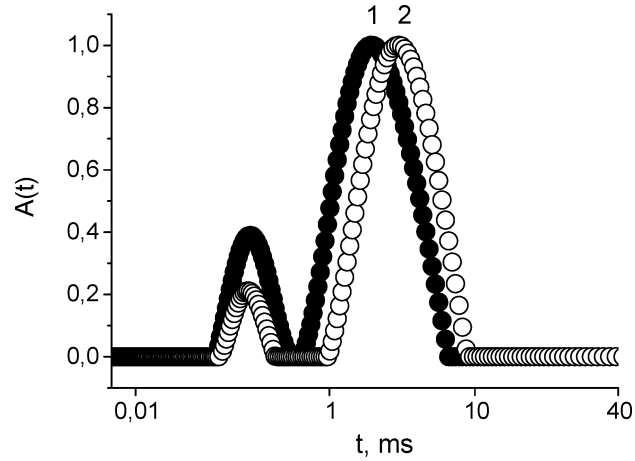

Figure 6. Distribution function of decay time $A(t)$ obtained by Contin method for 0.4 g/L aqueous solutions of chitosan (1) and HM chitosan (2) with molecular weight of 125 000 g/mol at scattering angle $\theta = 90°$. Solvent: 0.3 M acetic acid/0.05 M sodium acetate.

of the hydrodynamic radius of chitosan chain in a good solvent with the formula[50]

$$R_h \approx P^{1/10} \cdot (3\pi/128)^{1/2} \cdot (2L \cdot l_p)^{1/2} \qquad (12)$$

and we got the value of $R_h = 41$ nm, which is close to the experimental value obtained in ref 6.

In the present Article, in the same solvent, we observe the coexistence of single chains and aggregates of chitosan, the single chains being much more compact (as in θ-solvent) and the A_2 value being smaller (on the order of 10^{-4} cm^3 g^{-2} mol). Our data are consistent with the results reported in ref 75, where the aggregates were first observed by DLS in dilute aqueous solutions of chitosan. In this Article, the sizes of single chains and aggregates are the same as in the present article (cf. Figure 1 in this Article and figure 5a in ref 75). The authors point out[75] that the results are reproducible and suggest a possible ordered organization of aggregates predetermined by a particular molecular conformation. One can suggest that the differences in the aggregation behavior of chitosan samples in the same solvent may depend on the average number of hydrophobic GlcNAc units as well as on their distribution along the chain.

Therefore, the results obtained show that being dissolved in aqueous solution chitosan may behave as an associating polyelectrolyte forming multichain aggregates.

HM Chitosan. If hydrophobic side chains are introduced in chitosan macromolecules, then one may expect the formation of two types of cross-links in multichains aggregates:[12] (1) hydrophobic micelle-like domains typical for different polyelectrolytes with hydrophobic side groups and (2) junction zones inherent to chitosan itself.

Estimating the effect of covalently bound hydrophobes on the aggregation behavior of chitosan let us compare the data for HM and unmodified chitosan. It was shown that for all samples under study independently of the presence of hydrophobic substituents, two types of particles are always present: unimers and aggregates. Figure 6 shows the typical hydrodynamic radii distribution for HM and unmodified chitosan samples of the same molecular weight. It is seen that in HM chitosan, the peak of unimers is much smaller. The results of careful estimation presented in Tables 2 and 5 show that upon introduction of hydrophobic side chains, the weight fraction of aggregates x increases; therefore, the weight fraction of unimers

Table 5. Hydrodynamic Radii of Unimers $R_{h\,uni}$ and Aggregates $R_{h\,agg}$ and the Weight Fraction of Aggregates x in Dilute Aqueous Solutions of HM Chitosan[a]

sample	n_d[b]	$R_{h\,uni\,exper}$ (nm)[c]	$R_{h\,uni\,theor}$ (nm)[d]	$R_{h\,agg}$ (nm)[c]	x[c]
HM chitosan 55	14	13 ± 2	13	180 ± 10	0.12
HM chitosan 70	17	14 ± 2	15	180 ± 10	0.15
HM chitosan 125	31	17 ± 2	20	180 ± 8	0.24

[a] Solvent: 0.3 M acetic acid/0.05 M sodium acetate. [b] Average number of *n*-dodecyl groups per chain. [c] Values are extrapolated to zero concentration of HM chitosan. [d] Theoretical estimates of the hydrodynamic radii R_h of coils of individual chitosan macromolecules under θ conditions.

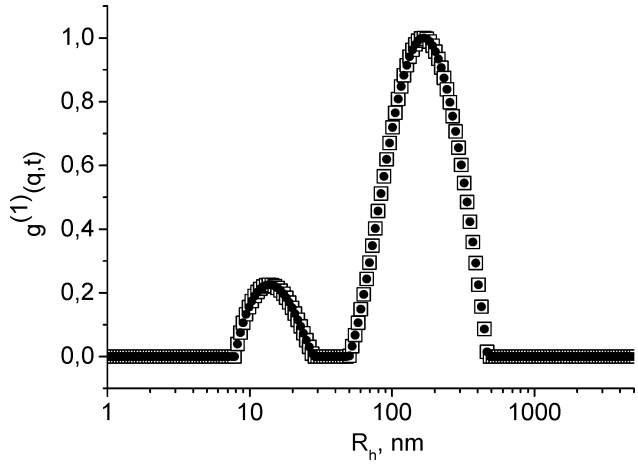

Figure 7. Distribution functions of hydrodynamic radii of HM chitosan (70 000 g/mol) obtained 1 h (□) and one month (●) after dissolution and filtration of the sample. The scattering angle θ is 90°. Solvent: 0.3 M acetic acid/0.05 M sodium acetate.

becomes smaller. This indicates that stronger hydrophobic interactions cause the unimers to associate.

For HM chitosan, the dependence of the ratio of the amplitude of fast and slow modes A_{fast}/A_{slow} of the electric field autocorrelation function on the polymer concentration is quite similar to that for unmodified chitosan (Figure 3), indicating that unimers and aggregates are in dynamic equilibrium.

To evaluate the role of aging on the aggregation, light scattering measurements were performed with solutions of HM chitosan at different intervals after polymer dissolution and filtration (10 min, 1 h, 24 h, 1 month). No changes were observed upon storage (Figure 7).

Let us compare the dimensions of single chains in HM and unmodified chitosan samples. Data presented in Tables 2 and 5 show that the hydrophobic modification does not affect appreciably the hydrodynamic radii of unimers. Most likely, the semirigid character of chitosan backbone and small number of hydrophobic substituents in a single chain make the intramolecular aggregation of hydrophobes unfavorable. Indeed, simple calculations show that spherical micelle-like domains with the radius of 15.4 Å (the contour length of *n*-dodecyl group) should contain ca. 40 *n*-dodecyl groups to avoid their unfavorable contact with water. In the polymers under study, the content of hydrophobic groups per chain is <40 (Table 5). Therefore, inside a single HM chitosan chain, we cannot expect the formation of stable micelle-like hydrophobic domains.

Now let us compare the size of aggregates in HM and unmodified chitosan. From Tables 2 and 5, it is seen that in HM chitosan the size of aggregates is much larger than that in its unmodified precursor. This fact suggests that the hydrophobic side groups of different polymer chains take part in the aggregation process. As in the case of unmodified chitosan, the

Table 6. Apparent Weight-Average Molecular Weight (M_w*), Apparent *z*-Average Radius of Gyration (R_g*), and Second Virial Coefficient A_2 Values Determined from Zimm Plots for Dilute Aqueous Solutions of HM Chitosan[a]

sample	M_w* (g/mol)	R_g* (nm)	A_2 (cm^3 mol/g^2)
HM chitosan 55	640 000	100 ± 5	3×10^{-4}
HM chitosan 70	770 000	100 ± 2	2×10^{-4}
HM chitosan 125	1 250 000	101 ± 4	1×10^{-4}

[a] Solvent: 0.3 M acetic acid/0.05 M sodium acetate.

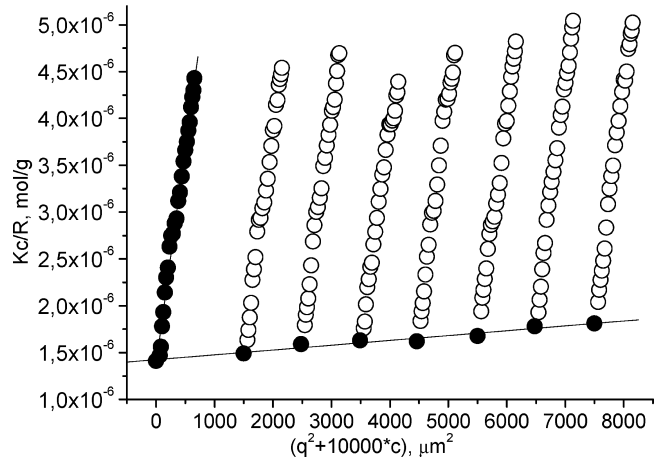

Figure 8. Zimm plot for aqueous solutions of HM chitosan (70 000 g/mol) in the range of polymer concentrations 0.1 to 0.8 g/L at scattering angles from 35 to 150° at 25 °C. Solvent: 0.3 M acetic acid/0.05 M sodium acetate.

hydrodynamic radii of aggregates in HM chitosan are independent of the length of individual chitosan chains, in agreement with theoretical predictions for associating polyelectrolytes.[17] To the best of our knowledge, before this study, such behavior was not observed experimentally for any associating polymer.

A typical Zimm plot of HM chitosan solutions is presented in Figure 8. It is seen that like in the case of unmodified chitosan the angular dependences of KC/R_θ are perfectly linear. The absence of curvature whatever the concentration in polymer is evidence that in this range aggregates are not concentration-dependent, which suggests a type of "closed" phenomenon of macromolecular association.[76]

The values of M_w*, R_g*, and A_2 obtained from the Zimm plots are listed in Table 6. Comparison of the data presented in Tables 3 and 6 shows that the second virial coefficient A_2 decreases when passing from chitosan to HM chitosan, which indicates that the solvent becomes poorer as a result of the incorporation of hydrophobic units in the polymer chain. Also, the apparent values of M_w* and R_g* for the HM chitosan are much higher than those for the corresponding unmodified samples. By using the same approach as that for unmodified chitosan, we estimated the values of the molecular weights of aggregates M_{agg}, their aggregation numbers N_{agg}, and radii of gyration $R_{g\,agg}$. The results are summarized in Table 7. It is seen that the M_{agg}, N_{agg}, and $R_{g\,agg}$ values in HM chitosan are always much higher than those in unmodified chitosan; that is, the incorporation of alkyl moieties into chitosan promotes the aggregation.

Similar to the case of chitosan itself, the aggregation numbers N_{agg} in HM chitosan decrease with increasing length of polymer backbone. As was mentioned above, this is due to smaller number of associating groups in shorter polymer chains, which requires the incorporation of larger number of chains in the aggregate to get a necessary gain in the energy of association.

Table 7. Characteristics of Aggregates in Dilute Aqueous Solutions of HM Chitosan[a]

sample	M_{agg} 10^6 g/mol	N_{agg}[b]	n_{agg}[c]	$R_{g\,agg}$ (nm)	$(R_g/R_h)_{agg}$	φ_{agg} 10^{-3}
HM chitosan 55	4.9	90 ± 20	30 000	106	0.59 ± 0.05	0.93
HM chitosan 70	4.7	70 ± 20	29 000	104	0.58 ± 0.05	0.94
HM chitosan 125	4.8	40 ± 10	29 400	105	0.58 ± 0.05	0.94

[a] Solvent: 0.3 M acetic acid/0.05 M sodium acetate. [b] Number of polymer chains. [c] Number of monomer units.

When this reason is the only one, the aggregation number should be just inversely proportional to the chain length of single macromolecules, which is indeed the case for HM chitosan (Table 7).

The decrease in the aggregation numbers with increasing length of individual macromolecules was previously observed for HM chitosan with associating cholesteryl side groups,[7] but no explanation was given for this effect. The values of the aggregation numbers in this Article are much smaller than those in our work: they drop from 40 (for polymer with MW of 5000 g/mol) to 2 (for polymer with MW of 200 000 g/mol), but the authors themselves consider these aggregation numbers N_{agg} to be only lower estimates of true N_{agg} because they are calculated just by dividing the diameter of aggregate by the diameter of single chain.[7] Larger values of aggregation numbers N_{agg} equal to 15−20 for HM chitosan (195 000 g/mol) bearing 2 mol % of *n*-octyl side groups were obtained in ref 32. They are consistent with our data if to take into account a smaller content of hydrophobes and higher molecular weight of the sample studied in this Article.

Table 7 shows that similar to the case of chitosan itself, the radii of gyration $R_{g\,agg}$ in HM chitosan are independent of the molecular weight (or the chain length) of unimer. Comparing the effect of the chain length of HM chitosan on the hydrodynamic $R_{h\,agg}$ (Table 5) or gyration radii of aggregates $R_{g\,agg}$ (Table 7) and on their aggregation numbers N_{agg} (Table 7), we come to the same conclusion as that for unmodified chitosan. When the chain length of individual macromolecules increases, the aggregates keep constant size ($R_{h\,agg}$ 180 nm, $R_{g\,agg}$ 105 nm), but their aggregation numbers N_{agg} drop from 90 to 40. Simple calculations show that despite quite different number of macromolecules in one aggregate (N_{agg}), the number of monomer units in each aggregate (n_{agg}) is roughly the same (Table 7). This means that polymer chains associate in such a way that independently of the chain length of individual macromolecules each aggregate contains a constant number of associating groups inducing the aggregation and a constant amount of charged groups counteracting the aggregation. As a result, the size of aggregates, which is determined only by the content of associating groups and charged units, is kept constant.

The values of the R_g/R_h ratio for the aggregates of HM chitosan, which might help to elucidate their structure, are shown in Table 7. It is seen that they are equal to 0.58 to 0.59, which is even lower than in unmodified chitosan (0.64 to 0.67). A similar small value of R_g/R_h (0.61) was previously observed by Buhler et al.[32] for aggregates of HM chitosan bearing 2 mol % of *n*-octyl side chains. Note that this value lies just between the R_g/R_h ratios for unmodified chitosan and HM chitosan with 4 mol % of *n*-dodecyl side chains. Buhler et al.[32] assign the observed small R_g/R_h value to the formation of intermolecularly bridged "flower-type" micelles. In our opinion, a more probable structure of the aggregate of HM chitosan (at least for the sample bearing 4 mol % of hydrophobes) is a nanogel structure with hydrophobic domains at the cross-links (Figure 9). In contrast with the model of intermolecularly bridged "flower-type" micelles, it suggests a negligibly small number of loops and a large number of chains interconnecting hydrophobic domains. Indeed, in our HM chitosan samples with 4 mol % of hydrophobic units randomly distributed along the backbone, the average contour length of the chain between two neighbor hydrophobic groups *l* is equal to ca. 120 Å when estimated as[77]

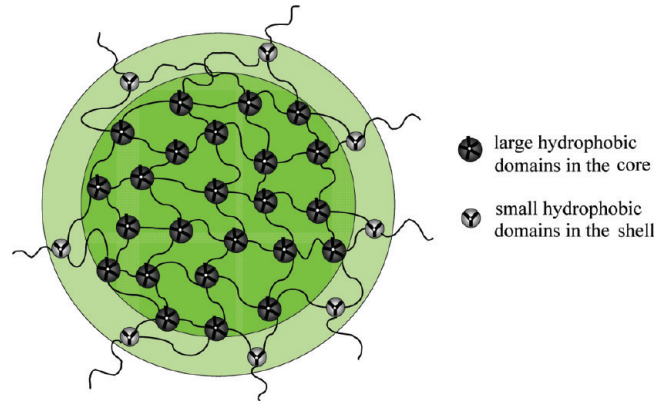

Figure 9. Schematic representation of multichain aggregate in aqueous solutions of HM chitosan. It consists of nanogel core covered with highly swollen shell with some dangling ends on the surface.

$$l = \sum_{\lambda=0}^{\infty} l_1 \lambda \nu (1-\nu)^{\lambda} = l_1(1-\nu)/\nu \qquad (13)$$

where ν is the mole fraction of hydrophobic units (0.04) and l_1 is the contour length of monomer unit (5.15 Å). Taking into account the fact that the persistence length of chitosan is ca. 75 Å,[14] it is difficult to imagine the back-folding of the 120 Å chain with the formation of loop.

The R_g/R_h ratio observed in aggregates of HM chitosan (0.58 to 0.59) lies within the range 0.3 to 0.6, which is characteristic[72,73,78] for microgels that have a surface layer with much lower density than the core and therefore a much larger hydrodynamic radius in comparison with the radius of gyration. Such highly swollen surface layer in HM chitosan aggregates may be due to two reasons. First, in the surface layer, the hydrophobic domains playing the role of cross-links can be much smaller than those in the core because of the lack of polymeric chains providing hydrophobes from the side of external solvent (Figure 9). Small content of hydrophobic units in the surface domains means that the surface layer is less dense. The existence of such surface layer (with the thickness on the order of subchain size) was theoretically suggested by Potemkin et al.[17] Second, one can expect the formation of dangling chains on the surface of nanogels. Indeed, HM chitosan chains containing only 4 mol % of hydrophobic grafts should have rather long chain ends free of hydrophobes. Most of these ends should be repelled from the aggregate because they do not carry any attractive sites; moreover, they possess many repulsive sites trying to escape similarly charged aggregate.

A somewhat similar model, "hydrophobically cross-linked chains", was proposed by Morishima et al.[79] for HM poly(sodium 2-acrylamido-2-methylpropanesulfonate) (HM PSAMPS) containing <3 mol % of hydrophobic dodecyl methacrylate units. In our model, in addition to "hydrophobically cross-linked chains" in the core, we suggest the presence of highly swollen surface layer (shell) covered by dangling ends.

Also, it should be emphasized that in contrast with aggregates of HM PSAMPS in HM chitosan nanogels, two types of cross-

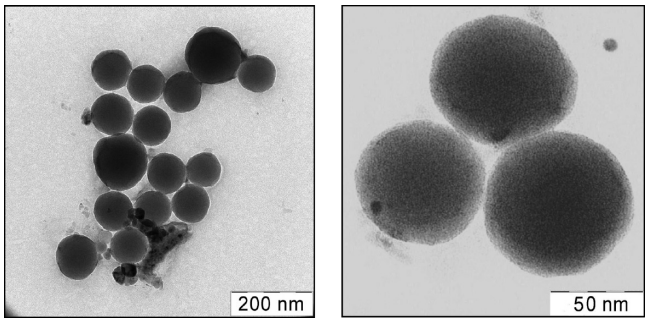

Figure 10. TEM micrographs of multichain aggregates of HM chitosan (70 000 g/mol).

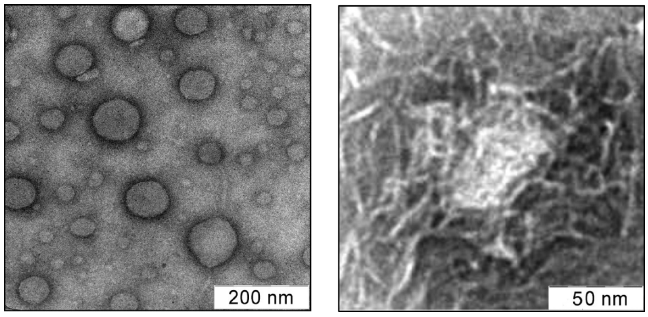

Figure 11. TEM micrographs of multichain aggregates of HM chitosan (70 000 g/mol) negatively stained with uranyl acetate.

links are expected: hydrophobic domains typical for any polyelectrolyte with hydrophobic side chains and hydrophobic domains (junction zones) inherent to chitosan itself.[12]

To check the suggestions about the form and structure of the aggregates of HM chitosan, we performed TEM experiments. The data obtained (Figures 10 and 11) show that the HM chitosan aggregates are of spherical shape and have an average radius of ca. 30−40 nm. Similar aggregates in shape and size were visualized by TEM for HM chitosan double-grafted with linoleic acid hydrophobic moieties and poly(β-malic acid) hydrophilic moieties.[80]

At the same time, in contrast with ref 80, our data (Figure 10) show that the aggregates have well-defined core−shell morphology. The thickness of the shell in the dried state, according to TEM data (Figure 10), is of ca. 10 nm, that is, 1/5 of the radius of the whole aggregate. Therefore, the TEM data seem to be consistent with LS results, indicating the core−shell nanogel structure of aggregates as depicted in Figure 9.

The values of the polymer volume fractions φ_{agg} inside the aggregates of HM chitosan are listed in Table 7. It is seen that they do not depend on the chain length of individual macromolecules and that they are 2.5 times higher than for aggregates of unmodified chitosan, which is expected taking into account the formation of additional cross-links. Nevertheless, the values of φ_{agg} remain rather low. These results are consistent with our model of "hairy" shell−core nanogel. Similar low polymer volume fractions φ_{agg} inside the aggregates of HM chitosan (10^{-3}) can be obtained by treating the data of ref 34.

Analyzing the results obtained, we can suggest the following picture of self-association of HM chitosan. The hydrophobic side chains tend to aggregate with each other. Because the content of hydrophobic groups in one macromolecule is not enough to form even one hydrophobic domain of optimum size, the groups belonging to different macromolecules are involved in the aggregation. It is reasonable to suggest that in the multichain aggregates that are formed hydrophobic domains are not identical. In the interior of the aggregate, the more energetically favorable ("strong") hydrophobic domains with an optimum content of hydrophobic groups are formed, whereas near the surface of the aggregate, the hydrophobic domains are smaller (and therefore weaker) because of the lack of neighboring chains providing hydrophobes at the boundary with the external solution. Therefore, for the most complete realization of hydrophobic attraction in the system, the aggregates should be as large as possible with the smaller fraction of "weak" hydrophobic domains in the surface layer. On the other hand, as a result of the intermolecular hydrophobic aggregation, the similarly charged repeat units of different polymeric chains are forced to come close to each other, which increases the electrostatic repulsion between them. In the interior of the aggregates the electrostatic repulsion is stronger because the charged units are surrounded by the similarly charged units from all the sides; in contrast, in the surface layer, the charged groups are exposed to water and thus the repulsive interactions for them are less pronounced. This means that from the point of view of electrostatic repulsion, the smaller aggregates with large total surface are favorable. Finally, as a result of competition of hydrophobic attraction leading to the growth of aggregates and electrostatic repulsion limiting their growth, the aggregates of optimum size are formed. So, the size of aggregates is determined only by the content of associating groups and charged units and does depend on the length of individual chains. To the best of our knowledge, this is the first observation of aggregates keeping a constant size independently of the length of individual chains in any associating polyelectrolyte solution.

Conclusions

Intermolecular association in dilute aqueous solutions of chitosan and HM chitosan of different molecular weights was studied by light scattering. It was observed that with increasing length of individual chains, the aggregates keep constant size and almost constant number of hydrophobic and charged units; simultaneously, the content of polymeric chains in one aggregate decreases. When comparing the association phenomena in chitosan and HM chitosan, one can conclude that the introduction of hydrophobic substituents leads to larger and denser aggregates with higher content of polymeric chains. Analysis of light scattering and TEM data suggests that in both chitosan and HM chitosan the aggregates can be regarded as highly swollen nanogels with more dense core and loose shell with some dangling chains on the surface. Unique combination of properties of chitosan (biocompatibility, biodegradability, positive charge, nontoxicity, and bioadhesiveness) makes such aggregates very promising for the use as nanosize drug carriers.

Acknowledgment. The financial support of the program "Scientific and Educational Staff of Innovative Russia" in 2009−2013 is gratefully acknowledged. We express our gratitude to Prof. I. I. Potemkin, Dr. E. A. Litmanovich and Dr. T. V. Laptinskaya for fruitful discussions and to Dr. S. S. Abramchuk for his help in TEM measurements.

References and Notes

(1) Ravi Kumar, M. N. V.; Muzzarelli, R. A. A.; Muzzarelli, C.; Sashiwa, H.; Domb, A. J. *Chem. Rev.* **2004**, *104*, 6017–6084.
(2) Sinha, V. R.; Singla, A. K.; Wadhawan, S.; Kaushik, R.; Kumria, R.; Bansal, K.; Dhawan, S. *Int. J. Pharm.* **2004**, *274*, 1–33.
(3) Rinaudo, M. *Prog. Polym. Sci.* **2006**, *31*, 603–632.
(4) Schatz, C.; Pichot, C.; Delair, T.; Viton, C.; Domard, A. *Langmuir* **2003**, *19*, 9896–9903.
(5) Lee, K. Y.; Jo, W. H.; Kwon, I. C.; Kim, Y.-H.; Jeong, S. Y. *Langmuir* **1998**, *14*, 2329–2332.

(6) Buhler, E.; Rinaudo, M. *Macromolecules* **2000**, *33*, 2098–2106.
(7) Kim, Y.-H.; Gihm, S. H.; Park, C. R.; Lee, K. Y.; Kim, T. W.; Kwon, I. C.; Chung, H.; Jeong, S. Y. *Bioconjugate Chem.* **2001**, *12*, 932–938.
(8) Liu, W.; Sun, S. J.; Zhang, X.; Yao, K. D. *J. Biomater. Sci., Polym. Ed.* **2003**, *14*, 851–859.
(9) Liu, W. G.; Zhang, X.; Sun, S. J.; Sun, G. J.; Yao, K. D.; Liang, D. C.; Guo, G.; Zhang, J. Y. *Bioconjugate Chem.* **2003**, *14*, 782–789.
(10) Matsumoto, T.; Kawai, M.; Masuda, T. *Biopolymers* **1991**, *31*, 1721–1726.
(11) Anthonsen, M. W.; Vårum, K. M.; Hermansson, A. M.; Smidsrød, O.; Brant, D. A. *Carbohydr. Polym.* **1994**, *25*, 13–23.
(12) Philippova, O. E.; Volkov, E. V.; Sitnikova, N. L.; Khokhlov, A. R.; Desbrieres, J.; Rinaudo, M. *Biomacromolecules* **2001**, *2*, 483–490.
(13) Schatz, C.; Pichot, C.; Delair, T.; Viton, C.; Domard, A. *Biomacromolecules* **2003**, *4*, 641–648.
(14) Lamarque, G.; Lucas, J.-M.; Viton, C.; Domard, A. *Biomacromolecules* **2005**, *6*, 131–142.
(15) Popa-Nita, S.; Alcouffe, P.; Rochas, C.; David, L.; Domard, A. *Biomacromolecules* **2010**, *11*, 6–12.
(16) Potemkin, I. I.; Vasilevskaya, V. V.; Khokhlov, A. R. *J. Chem. Phys.* **1999**, *111*, 2809–2817.
(17) Potemkin, I. I.; Andreenko, S. A.; Khokhlov, A. R. *J. Chem. Phys.* **2001**, *115*, 4862–4872.
(18) Jameela, S. R.; Jayakrishnan, A. *Biomaterials* **1995**, *16*, 769–775.
(19) Genta, I.; Constantini, M.; Asti, A.; Conti, B.; Montanari, L. *Carbohydr. Polym.* **1998**, *36*, 81–88.
(20) Monteiro, O. A. C.; Airoldi, C. *Int. J. Biol. Macromol.* **1999**, *26*, 119–128.
(21) Mi, F.-L.; Kuan, C.-Y.; Shyu, S.-S.; Lee, S.-T.; Chang, S.-F. *Carbohydr. Polym.* **2000**, *41*, 389–396.
(22) Crescenzi, V.; Francescangeli, A.; Taglienti, A.; Capitani, D.; Mannina, L. *Biomacromolecules* **2003**, *4*, 1045–1054.
(23) Lehr, C.; Bouwstra, J. A.; Schacht, E. H.; Junginger, H. E. *Int. J. Pharm.* **1992**, *78*, 43–48.
(24) He, P.; Davis, S. S.; Illum, L. *Int. J. Pharm.* **1998**, *166*, 75–88.
(25) Liu, X. F.; Guan, Y. L.; Yang, D. Z.; Li, Z.; Yao, K. D. *J. Appl. Polym. Sci.* **2001**, *79*, 1324–1335.
(26) Ikinci, G.; Şenel, S.; Akincibay, H.; Kaş, S.; Erciş, S.; Wilson, C. G.; Hincal, A. A. *Int. J. Pharm.* **2002**, *235*, 121–127.
(27) Dhawan, S.; Singla, A. K.; Sinha, V. R. *AAPS PharmSciTech* **2004**, *5*, 67.
(28) Philippova, O. E.; Akitaya, T.; Mullagaliev, I. R.; Khokhlov, A. R.; Yoshikawa, K. *Macromolecules* **2005**, *38*, 9359–9365.
(29) Kabanov, A. V.; Kabanov, V. A. *Bioconjugate Chem.* **1995**, *6*, 7–20.
(30) Aranaz, I.; Harris, R.; Heras, A. *Curr. Org. Chem.* **2010**, *14*, 308–330.
(31) Lee, K. Y.; Jo, W. H.; Kwon, I. C.; Kim, Y.-H.; Jeong, S. Y. *Macromolecules* **1998**, *31*, 378–383.
(32) Esquenet, C.; Buhler, E. *Macromolecules* **2001**, *34*, 5287–5294.
(33) Liu, C.-G.; Desai, K. G. H.; Chen, X.-G.; Park, H.-J. *J. Agric. Food Chem.* **2005**, *53*, 437–441.
(34) Jiang, G.-B.; Quan, D.; Liao, K.; Wang, H. *Mol. Pharmaceutics* **2006**, *3*, 152–160.
(35) Jiang, G.-B.; Quan, D.; Liao, K.; Wang, H. *Carbohydr. Polym.* **2006**, *66*, 514–520.
(36) Wang, Y. S.; Liu, L. R.; Jiang, Q.; Zhang, Q.-Q. *Eur. Polym. J.* **2007**, *43*, 43–51.
(37) You, J.; Hu, F.-Q.; Du, Y.-Z.; Yuan, H. *Biomacromolecules* **2007**, *8*, 2450–2456.
(38) Li, Y. Y.; Chen, X. G.; Liu, C. S.; Cha, D. S.; Park, H. J.; Lee, C. M. *J. Agric. Food Chem.* **2007**, *55*, 4842–4847.
(39) Ortona, O.; D'Errico, G.; Mangiapia, G.; Ciccarelli, D. *Carbohydr. Polym.* **2008**, *74*, 16–22.
(40) Rinaudo, M.; Auzely, R.; Vallin, C.; Mullagaliev, I. *Biomacromolecules* **2005**, *6*, 2396–2407.
(41) Rinaudo, M.; Le Dung, P.; Gey, C.; Milas, M. *Int. J. Biol. Macromol.* **1992**, *14*, 122–128.
(42) Plisko, E. A.; Nud'ga, L. A.; Danilov, S. N. *Russ. Chem. Rev.* **1977**, *46*, 764–774.
(43) Denuziere, A.; Ferrief, D.; Domard, A. *Carbohydr. Polym.* **1996**, *29*, 317–323.
(44) Rinaudo, M.; Milas, M.; Dung, L. P. *Int. J. Biol. Macromol.* **1993**, *15*, 281–285.
(45) Desbrieres, J.; Martinez, C.; Rinaudo, M. *Int. J. Biol. Macromol.* **1996**, *19*, 21–28.
(46) Moore, S.; Stein, W. H. *J. Biol. Chem.* **1948**, *176*, 367–388.
(47) Moore, S. *J. Biol. Chem.* **1968**, *243*, 6281–6283.
(48) Prochazkova, S.; Vårum, K. M.; Ostgaard, K. *Carbohydr. Polym.* **1999**, *38*, 115–122.
(49) Rinaudo, M.; Desbrieres, J.; Pavlov, G. *Polymer* **1999**, *40*, 7029–7032.
(50) Grosberg, A. Yu.; Khokhlov, A. R. *Statistical Physics of Macromolecules*; American Institute of Physics Press: New York, 1994; pp 10 and 21.
(51) Zimm, B. H. *J. Chem. Phys.* **1948**, *16*, 1099–1116.
(52) Provencher, S. W. *Macromol. Chem.* **1979**, *180*, 201–209.
(53) Nordmeier, E. *J. Phys. Chem.* **1993**, *97*, 5770–5785.
(54) Kuroda, K.; Fujimoto, K.; Sunamoto, J.; Akiyoshi, K. *Langmuir* **2002**, *18*, 3780–3786.
(55) Blagodatskikh, I. V.; Vasil'eva, O. V.; Ivanova, E. M.; Bykov, S. V.; Churochkina, N. A.; Pryakhina, T. A.; Smirnov, V. A.; Philippova, O. E.; Khokhlov, A. R. *Polymer* **2004**, *45*, 5897–5904.
(56) Akiyama, E.; Morimoto, N.; Kujawa, P.; Ozawa, Y.; Winnik, F. M.; Akiyoshi, K. *Biomacromolecules* **2007**, *8*, 2366–2373.
(57) Filippov, S. K.; Lezov, A. V.; Sergeeva, O. Yu.; Oliferenko, A. S.; Lesnichin, S. B.; Domnina, N. S.; Komarova, E. A.; Almgren, M.; Karlsson, G.; Štepanek, P. *Eur. Polym. J.* **2008**, *44*, 3361–3369.
(58) Gao, J.; Haidar, G.; Lu, X.; Hu, Z. *Macromolecules* **2001**, *34*, 2242–2247.
(59) Braccini, I.; Rodriguez-Carvajal, M. A.; Perez, S. *Biomacromolecules* **2005**, *6*, 1322–1328.
(60) Jordan, R. C.; Brant, D. A. *Biopolymers* **1978**, *17*, 2885–2895.
(61) Davis, M. A. F.; Gidley, M. J.; Morris, E. R.; Powell, D. A.; Rees, D. A. *Int. J. Biol. Macromol.* **1980**, *2*, 330–332.
(62) Kravtchenko, T. P.; Berth, G.; Voragen, A. G. J.; Pilnik, W. *Carbohydr. Polym.* **1992**, *18*, 253–263, and references therein.
(63) Rolland-Sabaté, A.; Mendez-Montealvo, M. G.; Colonna, P.; Planchot, V. *Biomacromolecules* **2008**, *9*, 1719–1730.
(64) Kawata, T.; Hashidzume, A.; Sato, T. *Macromolecules* **2007**, *40*, 1174–1180.
(65) Liu, R. C. W.; Pallier, A.; Brestaz, M.; Pantoustier, N.; Tribet, C. *Macromolecules* **2007**, *40*, 4276–4286.
(66) Rayleigh, L. *Philos. Mag.* **1882**, *14*, 182.
(67) Zhou, Z.; Peiffer, D. G.; Chu, B. *Macromolecules* **1994**, *27*, 1428–1433.
(68) Zhang, Y.; Wu, C.; Fang, C.; Zhang, Y.-X. *Macromolecules* **1996**, *29*, 2494–2497.
(69) Savin, G.; Burchard, W.; Luca, C.; Beldie, C. *Macromolecules* **2004**, *37*, 6565–6575.
(70) Errington, N.; Harding, S. E.; Vårum, K. M.; Illum, L. *Int. J. Biol. Macromol.* **1993**, *15*, 113–117.
(71) Berth, G.; Cölfen, H.; Dautzenberg, H. *Prog. Colloid Polym. Sci.* **2002**, *119*, 50–57.
(72) Burchard, W. *Adv. Polym. Sci.* **1999**, *143*, 113–194.
(73) Burchard, W. *Adv. Polym. Sci.* **1983**, *48*, 1–124.
(74) Terbojevich, M.; Cosani, A.; Conio, G.; Marsano, E.; Bianchi, E. *Carbohydr. Res.* **1991**, *209*, 251–260.
(75) Sorlier, P.; Rochas, C.; Morfin, I.; Viton, C.; Domard, A. *Biomacromolecules* **2003**, *4*, 1034–1040.
(76) Elias, H.-G. In *Light Scattering from Polymer Solutions*; Huglin, M. B., Ed.; Academic Press: New York, 1972; Ch. 9.
(77) Hyunmin, Y.; Wu, L.-Q.; Bentley, W. E.; Ghodssi, R.; Rubloff, G. W.; Culver, J. N.; Payne, G. F. *Biomacromolecules* **2005**, *6*, 2881–2894.
(78) Schmidt, M.; Nerger, D.; Burchard, W. *Polymer* **1979**, *20*, 582–592.
(79) Noda, T.; Morishima, Y. *Macromolecules* **1999**, *32*, 4631–4640.
(80) Zhao, Z.; He, M.; Yin, L.; Bao, J.; Shi, L.; Wang, B.; Tang, C.; Yin, C. *Biomacromolecules* **2009**, *10*, 565–572.

BM100990U